Tectonophysics 583 (2013) 124–130

Contents lists available at SciVerse ScienceDirect

Tectonophysics

journal homepage: www.elsevier.com/locate/tecto

Rheology of synthetic polycrystalline halite in torsion

F.O. Marques *, J.-P. Burg, M. Armann, E. Martinho

Department of Geosciences, Swiss Federal Institute of Technology (ETH-Zürich), CH-8092 Zurich, Switzerland

ARTICLE INFO

Article history:
Received 23 June 2012
Received in revised form 5 October 2012
Accepted 24 October 2012
Available online 31 October 2012

Keywords:
Halite/rock salt
Rheology
Microstructure
Halite strength
Torsion experiments

ABSTRACT

Motivated by the need for halite rheology, we investigated the stress/strain/strain rate behaviour of halite to high shear strains in torsion, using polymer jackets whose strength does not influence halite rheology. The experimental results show that: (1) halite strength decays exponentially with temperature increase, being very weak at 300 °C (ca. 2 Nm); (2) power-laws fit the stress/strain rate data, from which we determined the stress exponent n between ca. 13 (60 °C) and ca. 3 (200 °C), indicating that n decreases exponentially with temperature increase; (3) the activation energy Q decreases exponentially with temperature increase, from ca. 159 kJ/mol (38 kcal/mol) at 60 °C to ca. 59 kJ/mol (14 kcal/mol) at 200 °C; (4) Q depends linearly on n with a slope of ca. 10. The empirical constitutive equation

$$\dot{\gamma} = 12.1\exp(9.6 + 7.1\text{E}{-}6\exp(1/T1.9\text{E}{-}4))\tau^{(2.5+9.3\text{E}6\exp(-T/24.3))}$$

describes the experimental results. Comparison of the present and previous experimental results shows that halite is much weaker in shear than in axial compression or extension. This difference likely results from the rotational component of simple shear.

1. Introduction

Halite has physical properties that are unique and make it a preferential target: low density, very low permeability, high ductility, low creep strength, high solubility and near incompressibility. Halite is also the major component of evaporites, which commonly occur as diapirs or salt walls. These salt deposits can play an important role in hydrocarbon trapping, and have become preferential targets for repository of gas and chemical/nuclear waste. Therefore, there is a great need for the knowledge of halite stress/strain/strain rate behaviour; this is why we carried out the present experimental study. We ran all experiments with very weak polymer jackets, because metal jackets mask halite's actual strength (Marques et al., 2010) and we do not need to correct measured values. In order to build up predictive capability that can help in engineering and modelling work, we developed an empirical constitutive equation that describes the macroscopic behaviour (continuum mechanics) of halite in the experiments.

Most previous work on halite rheology has been carried out under extension, compression or indentation, whether on single or polycrystalline, natural or synthetic halite, in a temperature range from room to 780 °C, and under a confining pressure from atmospheric to 250 MPa (e.g. Carter and Hansen, 1983; Carter et al., 1993; Davidge and Pratt, 1964; Franssen, 1994; Gangi, 1983; Horseman and Handin, 1990; Ter Heege et al., 2005; Urai et al., 1986; Wawersik and Zeuch, 1986). High strain is common in deformed rock salt, but not in axial compression/extension tests; therefore, we investigated the mechanical behaviour of halite under torsion, up to shear strains of $\gamma \approx 6$.

2. Materials and methods

2.1. Sample preparation

The NaCl used in this study was obtained from the company AppliChem. The salt was delivered as an analytical fine-grained powder with a grain size of ~500 μm. According to the supplier, the purity is 99.9% with traces of bromide, iodide, and sulphate, and with cations of Ba, Ca, Fe, K, Mg and Pb. The powder was filled, in single portions of 30 ml each, into a stainless steel cylinder with a diameter of 50 mm and a length of 250 mm. The metal container was enclosed by two tightly screwed stainless steel plates from the sides. The powder filling was, at each step, uniaxially pressed by a load of 40×10^3 kg, for 20 s, on a surface of ca. 1.96×10^{-3} m^2, which corresponds to ca. 200 MPa. This procedure was repeated until the cylinder was completely filled. Finally, the material inside the cylinder was uniaxially cold pressed by a load of 30×10^3 kg (ca. 150 MPa) for 1 h. After this final cold pressing, the cylinder was sealed from top to bottom by two additional steel pieces. All parts were screwed

* Corresponding author at: University of Lisbon, Portugal. Tel.: +351 217500000; fax: +351 217500064.
E-mail address: fomarques@fc.ul.pt (F.O. Marques).

0040-1951/$ – see front matter © 2012 Elsevier B.V. All rights reserved.
http://dx.doi.org/10.1016/j.tecto.2012.10.024

tightly together to keep the material under the applied confining pressure. The assembly was then placed in an oven for one week at 200 °C. Because of sample compaction, and in order to keep the confining pressure, the screws were tightened twice a day.

After this procedure, the starting material showed an isotropic polygonal microstructure of halite crystals with grain-size between 150 and 300 μm. Using a pycnometer, we measured the density of this starting material (ca. 2150 kg m^{-3}), which indicates a porosity of ca. 0.6%. The water content was ca. 35 ppm, as determined by FTIR (Armann, 2008). Cylindrical samples 15 mm in diameter were cored and oven-dried at 110 °C and atmospheric pressure for at least 24 h before testing.

The preparation of the deformed samples for microscopy was as follows. The polishing was carried out dry, using first 1200 grid SIC polishing paper. After that, the samples with the polished surface were embedded in resin with hardener. The embedded samples were stored for 24 h in a vacuum oven for the resin to dry. Afterwards the samples were polished again, but now polishing was carried out wet, using evaporating oil as a lubricant. The first polishing was carried out with 1200 grid SIC paper to remove the resin layer, after which a 2500 grid SIC paper was used to remove the scratches from the first polishing. Final polishing was done with 4000 grid SIC paper to reveal a nearly scratch-free surface. Between the different polishing steps the surface was cleaned by using evaporating oil to remove the polishing particles from the surface. The sample was then cleaned with compressed air and then flushed with n-Hexane containing some MgO crystals to bind the water in the n-Hexane. Cleaning was done to remove leftover evaporating oil. Then the sample was held horizontally and the etching solution (95% saturated NaCl solution containing 8 wt.% $FeCl_3 \times 6H_2O$) was placed on the entire surface for 4 s. After the 4 s, the surface was flushed immediately with n-Hexane and dried by using a hair dryer. Etching is necessary to highlight the grain and sub-grain boundaries and to obtain a surface layer free of defects introduced during mechanical polishing.

2.2. Deformation apparatus and boundary conditions

The experiments were conducted in a Paterson rig, an apparatus based on a standard gas-medium, high-pressure and high-temperature triaxial deformation machine, on which an additional module allows rotary shear of a cylindrical specimen (Paterson and Olgaard, 2000). In torsion experiments, approximated simple shear deformation occurs locally at any given position in the sample. The shear strain γ and shear strain rate $\dot{\gamma}$ increase linearly from zero along the central axis of the sample to a maximal value at the outer circumference. $\dot{\gamma}$ at any radius can be calculated from the angular displacement rates using Eq. (3) in Paterson and Olgaard (2000). The mentioned experimental γ and $\dot{\gamma}$ are the maximal values applied at the outer rim of the cylindrical specimen. The temperature distributions were regularly calibrated so that the temperature variation across the sample was never more than 2 °C. The experiments were conducted at 60, 100, 200 and 300 °C, at 250 MPa confining pressure and at constant angular displacement rate corresponding to a $\dot{\gamma} = -4\,s^{-1}$ up to $\gamma = 6$.

Strain rate stepping (SRS) tests ($\dot{\gamma}$ from 1E-5 s^{-1} to 2E-3 s^{-1}) were run to determine the dependence of flow strength on $\dot{\gamma}$. The response of the internal torque M to a variation in angular displacement rate yields the stress exponent n, which gives an indication of the active deformation mechanism. The measured internal torque can be converted to shear stress τ assuming power-law creep behaviour. The shear stress determination is based on the assumptions of a cylindrical sample shape and a unique deformation mechanism controlling deformation throughout the sample.

The results of testing by Marques et al. (2010) indicate that Polyethylene (PE) and Polytetrafluorethylene (PTFE) are the most appropriate materials to serve as soft jackets for temperatures <150 °C and <300 °C, respectively. Therefore, the jackets used in the present experiments were machined from PE and PTFE rods.

3. Experimental results

3.1. Rheology

3.1.1. Torque/twist data

Torque/strain data for 60, 100, 200 and 300 °C are plotted in Fig. 1. At 60 °C, yielding was followed by strain hardening, steep until $\gamma \approx 1$ and then shallower until jacket failure. At 100 °C, yielding was followed by strain hardening, then by a plateau that lasted for about $\gamma \approx 1$ (transient steady state creep), which in turn was followed by hardening until jacket failure. At 200 °C, yield was followed by short-term hardening, which in turn was followed by constant stress flow until the experiment was arrested. At 300 °C, yield was immediately followed by constant stress flow. At all temperatures except 300 °C, yield was followed by strain hardening, whose steepness gradually decreased with temperature, thus making yield more apparent at higher temperatures. The graph in Fig. 2 summarizes halite strength at different temperatures and similar strain ($\gamma\gamma \approx 2$) and shows that strength decreases exponentially with temperature (fit with $R^2 = 0.999$).

3.1.2. Strain rate stepping (SRS) tests

The SRS test could not be performed at 300 °C because the strength of halite was below 1 Nm at this temperature and at the applied lower strain rates. At 60, 100 and 200 °C, data points are fit by power laws ($R^2 > 0.99$).

At 60 and 100 °C, data points are fit by single straights in the Log × Log graph of Fig. 3, and $n \approx 13.2$ and $n \approx 4.2$ can be calculated. At 200 °C, a single straight still fits the data points, and $n \approx 2.8$; however, a better fit can be obtained if low and high strain rate points are considered separately, yielding $n \approx 2.6$ and 4.1 respectively.

As shown in the graph of Fig. 4, n decays exponentially with increasing temperature. Data in Heard (1972, Table 1) also indicate a dependence of n on temperature, especially at temperatures below 200 °C ($n \approx 16.6$, 12.7 and 5.0 at 23, 100 and 200 °C, respectively), as in the present experiments.

3.2. Microstructure

Microstructures developed in the deformed samples depended on temperature and amount of shear strain. Samples deformed at 100 °C and $\gamma < 3$ (Fig. 5A) showed stretched grains whose gross shape and orientation were close to the corresponding finite strain ellipse. In general, these grains had serrated boundaries, and contained blocky

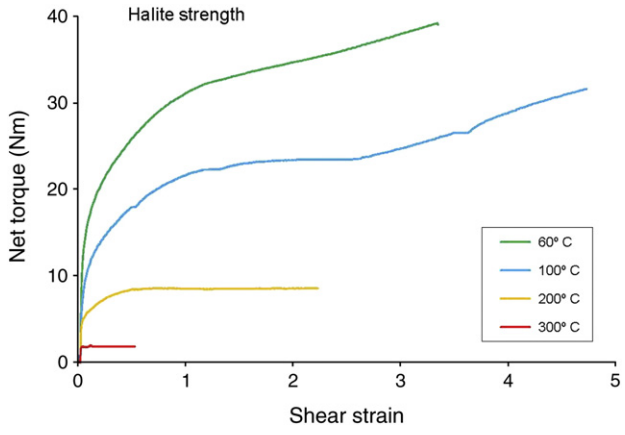

Fig. 1. Torque/strain graph to show halite strength at 60, 100, 200 and 300 °C. Note that constant stress flow is reached very early at 200 and, especially, 300 °C.